AGU PUBLICATIONS

JGR

Journal of Geophysical Research: Space Physics

RESEARCH ARTICLE
10.1002/2017JA024730

Special Section:
Dayside Magnetosphere Interaction

How Much Flux Does a Flux Transfer Event Transfer?

R. C. Fear[1], L. Trenchi[1,2], J. C. Coxon[1], and S. E. Milan[3]

[1]Department of Physics & Astronomy, University of Southampton, Southampton, UK, [2]Now at ESRIN, European Space Agency, Frascati, Italy, [3]Department of Physics and Astronomy, University of Leicester, Leicester, UK

Key Points:
- There is an order-of-magnitude discrepancy between in situ/ionospheric estimates of FTE flux transfer
- This discrepancy arises due to implicit assumptions made about FTE structure
- Removing these assumptions reveals that FTEs could be the major driver of magnetospheric convection

Correspondence to:
R. Fear,
R.C.Fear@soton.ac.uk

Citation:
Fear, R. C., Trenchi, L., Coxon, J. C., & Milan, S. E. (2017). How much flux does a flux transfer event transfer? *Journal of Geophysical Research: Space Physics*, *122*. https://doi.org/10.1002/2017JA024730

Received 31 AUG 2017
Accepted 15 NOV 2017
Accepted article online 20 NOV 2017

Abstract Flux transfer events are bursts of reconnection at the dayside magnetopause, which give rise to characteristic signatures observed by a range of magnetospheric/ionospheric instrumentation. One outstanding problem is that there is a fundamental mismatch between space-based and ionospheric estimates of the flux that is opened by each flux transfer event—in other words, their overall significance in the Dungey cycle. Spacecraft-based estimates of the flux content of individual flux transfer events (FTEs) correspond to each event transferring flux equivalent to approximately 1% of the open flux in the magnetosphere, whereas studies based on global-scale radar and auroral observations suggest this figure could be of the order of 10%. In the former case, flux transfer events would be a minor detail in the Dungey cycle, but in the latter they could be its main driver. We present observations of two conjunctions between flux transfer events observed by the Cluster spacecraft and pulsed ionospheric flows observed by the Super Dual Auroral Radar Network (SuperDARN) network. In both cases, a similar number of FTE signatures were observed by Cluster and one of the SuperDARN radars, but the conjunctions differ in the azimuthal separation of the spacecraft and ionospheric observations (i.e., the distance of the spacecraft from the cusp throat). We argue that the reason for the existing mismatch in flux estimates is due to implicit assumptions made about FTE structure, which tacitly ignore the majority of flux opened in mechanisms based on longer reconnection lines. If the effects of such mechanisms are considered, a much better match is found.

Plain Language Summary The Earth's magnetosphere is the highly dynamic region of space occupied by the Earth's magnetic field. Its dynamics are driven by its interaction with the solar wind, through a process called "magnetic reconnection," in which magnetic fields from the Sun and the Earth interconnect. Reconnection occurs in bursts called "flux transfer events" that cause signatures that can be seen by both spacecraft and ionospheric radars. Either type of measurement can be used to work out the amount of magnetic reconnection occurring in each burst, but the two methods produce very different results. In this paper we show that a consistent answer can be obtained from both methods, but a new approach must be taken with the spacecraft observations. Our results suggest that flux transfer events could be the main driver of the magnetosphere's dynamics.

1. Introduction

It was first proposed by Dungey (1961) that the dynamics of Earth's magnetosphere were primarily driven by magnetic reconnection. The first direct observation of the accelerated flows predicted by reconnection at the Earth's magnetopause was made by Paschmann et al. (1979), but these observations were shortly preceded by evidence of observational signatures termed "flux erosion events" (Haerendel et al., 1978) or "flux transfer events" (Russell & Elphic, 1978, 1979) (subsequently shown to be equivalent; Rijnbeek & Cowley, 1984). Flux transfer events (FTEs) were identified as signatures of transient reconnection; their characteristic feature is a bipolar variation in the component of the magnetic field normal to the magnetopause, B_N (see also Rijnbeek et al., 1982; Russell & Elphic, 1978, 1979), but in situ signatures also include either an enhancement or sometimes a "crater" signature in the magnetic field strength (Farrugia et al., 1988, 2011; Paschmann et al., 1982; Owen et al., 2008) and mixing of the plasma populations from either side of the magnetopause (Daly et al., 1981, 1984; Thomsen et al., 1987).

There exist also ionospheric signatures of FTEs, which form at the footprints of newly opened magnetic field lines. These signatures can be observed optically as Poleward Moving Auroral Forms (PMAFs; Sandholt et al., 1986, 1992), and in radar data as Pulsed Ionospheric Flows or Poleward Moving Radar Auroral Forms

Table 1
Observational Estimates of Flux Content of FTEs

Study	Type of data	Flux estimate	Percentage of polar cap opened by one event[a]
Russell and Elphic (1979)	Spacecraft case study	22 MWb, 29 MWb	4–5%
Saunders et al. (1984)	Spacecraft case study	4 MWb	0.7%
Rijnbeek et al. (1984)	Spacecraft statistical study	3 MWb	0.5%
Hasegawa et al. (2006)[b]	Spacecraft Grad Shafranov reconstructions	1–4 MWb	0.2–0.7%
Zhang et al. (2008)	Fit of spacecraft observations to model	0.4 MWb	0.07%
Eastwood et al. (2012)	Force-free fit of spacecraft observations	0.8–3 MWb	0.1–0.5%
Lockwood et al. (1990)	Simultaneous auroral/radar case studies	7–34 MWb	1–6%
Milan et al. (2000)	Global-scale auroral/radar case study	75 MWb[c]	13%
Marchaudon, Cerisier, Greenwald, et al. (2004); Marchaudon, Cerisier, Bosqued, et al. (2004)	Radar case studies	1 MWb, 5 MWb[c]	0.2–0.8%
Oksavik et al. (2005)	Radar case study	1 MWb (minimum)	>0.2%
This study	Conjugate spacecraft/global-scale radar case study	77 ± 26, 46 ± 25 MWb[d]	8–13%

[a]Assuming a typical polar cap flux content of 600 MWb (Milan et al., 2007; Huang et al., 2009). [b]Includes also reanalysis of an FTE reconstructed by Sonnerup et al. (2004), who also determined a flux of 2 MWb. [c]Calculated from quoted value of area of polar cap opened by each event and ionospheric magnetic field strength of 5×10^4 nT. [d]Values refer to the radar and spacecraft estimates for the FTEs in Event 1 (for which the X line extent is estimated).

(McWilliams et al., 2000; Milan, Lester, et al., 1999; Pinnock et al., 1993, 1995; Provan et al., 1998, 1999; Provan & Yeoman, 1999; Rae et al., 2004). Conjugate studies have shown the link between spacecraft and ionospheric signatures of FTEs (Amm et al., 2005; Elphic et al., 1990; McWilliams et al., 2004; Wild et al., 2001, 2003, 2005, 2007), between optical and radar FTE signatures (Moen et al., 1995; Milan, Cowley, et al., 1999), and in occasional case studies, simultaneous observations of all three (Neudegg et al., 2001). Neudegg et al. (2000) reported the results of a statistical study of in situ signatures of FTEs observed by the Equator-S spacecraft and associated flow bursts in the ionosphere observed by the Super Dual Auroral Radar Network (SuperDARN) HF radars; they noted the difficulty sometimes present in finding a one-to-one association between individual satellite FTE signatures and individual ionospheric signatures, and therefore, in their survey they collated groups of signatures. They found that 77% of in situ FTE signatures (or groups of signatures) were associated with an ionospheric flow signature (or groups of flow signatures), and 64% of their identified ionospheric flow events were associated with an in situ FTE signature (or group of signatures). However, some of the case studies examined by Neudegg et al. (2000) and in subsequent studies (e.g., Wild et al., 2001, 2003) found a clearer one-to-one correlation between individual in situ FTE signatures and their ionospheric counterparts.

Several studies have made estimates of the flux content of flux transfer events, and by comparing these to the average amount of open flux in the magnetospheric system, we can infer an estimate of their overall significance to the Dungey cycle. Table 1 summarizes some of the flux estimates made observationally. Different approaches have been taken; several studies make observational estimates of the dimensions of the flux rope, either from case studies (Russell & Elphic, 1979; Saunders et al., 1984) or based on statistical arguments (Rijnbeek et al., 1984), which is then multiplied by the peak field strength to obtain the total flux. Sonnerup et al. (2004) and Hasegawa et al. (2006) reconstructed the spatial structures of FTEs from time series observations using the Grad Shafranov technique and reported the flux mapping through the reconstructed FTEs, whereas Zhang et al. (2008) and Eastwood et al. (2012) estimated the flux content of an FTE by fitting spacecraft observations to flux rope models (the Kivelson & Khurana 1995 and force-free models, respectively) and calculating the total flux content from the model. All of the above flux estimates are derived from spacecraft data and give rise to estimates of flux transfer that generally range from 0.4 to 4 MWb, which corresponds to each event opening flux equivalent to between 0.1 and 1% of the flux typically contained in the polar cap (Table 1).

The Russell and Elphic (1979) flux calculations are outliers amongst the spacecraft-based estimates, reporting flux estimates of 22 MWb and 29 MWb, which would equate to 4–5% of the polar cap being opened in each event. These estimates assume a circular cross section and for a core field of 50 nT equate to a flux rope radius of 2.1 R_E, which appears large compared with statistical estimates of spatial scale both normal

to the magnetopause (Rijnbeek et al., 1984) and along the magnetopause in the direction of the FTE velocity (Fear et al., 2007). Furthermore, Russell and Elphic (1979) also noted that an alternative plasma instrument on the same spacecraft provided velocity measurements that were lower and would correspond to flux calculations that were a factor of 2 less. Therefore, although Russell and Elphic (1979) argued that their estimates should be treated as a lower limit to the true *total* rate of reconnection at the time (due to the possibility of missed events if the satellite was poorly situated), we argue that their estimates should be considered as being an upper limit of the flux estimates *per event* that can reasonably be derived in this way from spacecraft observations. Given the mean repetition rate of FTE signatures of ~8 min (Lockwood & Wild, 1993; Rijnbeek et al., 1984) and taking a typical cross polar cap convection time of ~2 h for moderately or strongly southward interplanetary magnetic field (IMF) conditions (Browett et al., 2017; Cowley, 1981; Fear & Milan, 2012; Rong et al., 2015; Zhang et al., 2015), in which time the polar cap is entirely refreshed, this implies that flux transfer events are typically capable of providing 1.5–15% of the flux transfer into the magnetotail; the implication of this estimate is that the balance is contributed by quasi-steady reconnection, in which case flux transfer events form a relatively minor part of the Dungey cycle (as argued by Newell & Sibeck, 1993, though their assumptions and conclusions were disputed by Lockwood et al., 1995).

Other studies have inferred the flux content of FTEs from ionospheric and auroral observations. Lockwood et al. (1990) estimated the longitudinal and latitudinal extent of a series of ionospheric flow channels using data from the European Incoherent Scatter radar (EISCAT), operating in a mode in which the beam was swung either side of the northward direction. By taking the product of the estimated area of the flow channel and the ionospheric magnetic field strength, they determined magnetic fluxes transferred by a series of individual FTEs that varied from 7 to 34 MWb; higher than all of the spacecraft estimates discussed above (though overlapping with the range calculated by Russell & Elphic 1979). Subsequent ionospheric studies (e.g., Marchaudon, Cerisier, Greenwald, et al., 2004; Marchaudon, Cerisier, Bosqued, et al., 2004; Oksavik et al., 2005) have reported values that are similar to either Lockwood et al. (1990) or the spacecraft estimates above. However, Milan et al. (2000), presenting global-scale observations of a sequence of poleward moving auroral forms observed by the Polar spacecraft Ultraviolet Imager and conjugate SuperDARN observations of radar PMAFs, reported that the polar cap area was increased by a far greater area than previously appreciated; based on the area increases quoted by Milan et al. (2000), the flux transfer can be inferred to be ~75 MWb for each event. If this is the case, then on the basis of the arguments above, we might expect the Dungey cycle to be entirely driven by FTEs (i.e., any contribution from quasi-steady state reconnection would be small). Milan et al. (2000) concluded that the discrepancy between their value and previous ionospheric estimates was because the full local time extent of ionospheric FTE signatures had not previously been appreciated. This conclusion explains the discrepancy between ionospheric estimates in Table 1, but only goes part way to explain the discrepancy between those values and spacecraft estimates. As will be discussed further in the following section, we argue that implicit assumptions are made about FTE structure that may lead to a significant underestimation of the total flux transfer. In this paper, we argue that previous spacecraft estimates have implicitly assumed the Russell and Elphic (1978) flux tube structure; we present a simple new method to estimate the total flux transferred by a flux transfer event using spacecraft observations (supported by ionospheric observations) by explicitly considering subsequently postulated structures based on longer reconnection lines (X lines). We show that this removes most of the discrepancy between spacecraft and ionospheric observations.

The outline of the paper is as follows. In section 2 we discuss the implications of FTE structure on flux estimates and present our proposed approach. We then outline the instrumentation (section 3) and observations used (section 4), before calculating what we propose is the true contribution of FTEs to the Dungey cycle (also section 4). We then discuss the significance of our results and conclude.

2. Methodology

The initial interpretation of in situ FTE signatures was that they arose due to an azimuthally narrow tube of reconnected flux (Russell & Elphic, 1978), whereas subsequent models were developed that incorporated a longer, coherent, X line that could be extended to any arbitrary length (Lee & Fu, 1985; Southwood et al., 1988; Scholer, 1988). These long X line mechanisms fall into two camps; Lee and Fu (1985) proposed that the flux rope observed could be formed by multiple X lines, whereas Southwood et al. (1988) and Scholer (1988) advocated a mechanism based on bursty reconnection at a single X line resulting in heating of plasma that

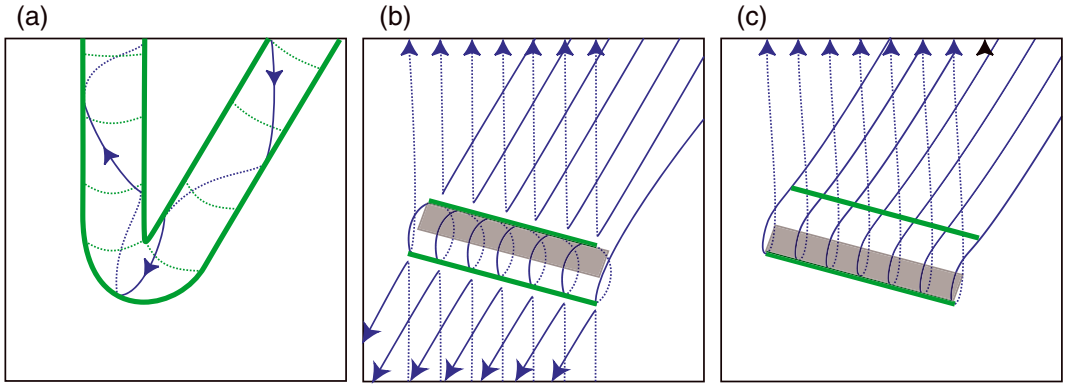

Figure 1. A cut-away version of Figure 1 in Fear et al. (2008), showing only the open field lines in three different FTE formation models: (a) Russell and Elphic (1978), (b) the multiple X line model (Lee & Fu, 1985), (c) the single X line model (Southwood et al., 1988; Scholer, 1988). The grey rectangles represent surfaces in the plane of the magnetopause that are discussed in section 2.

causes a bulge in the magnetopause boundary layer, giving rise to the same characteristics. (See section 2 and Figure 1, specifically, of Fear et al., 2008 for a more extensive summary.) Lockwood et al. (1990) noted that these longer X line models have the effect of multiplying the estimated flux by a factor roughly equal to the ratio of the length of the reconnection line to the diameter of the Russell and Elphic (1978) flux tube. Furthermore, Fear et al. (2008) noted that in the multiple X line mechanism (Lee & Fu, 1985), most of the flux that was opened by the flux transfer event did not actually map through the flux rope, and that most of the ionospheric signature was therefore due to the flux opened by the reconnection burst, which did not map through the flux rope observed by spacecraft. This is illustrated in Figure 1, which shows sketches of the (a) Russell and Elphic (1978), (b) multiple X line (Lee & Fu, 1985), and (c) single X line (Southwood et al., 1988; Scholer, 1988) FTE models, viewed looking down onto the plane of the magnetopause. This figure is based on Figure 1 in Fear et al. (2008), but the overdraped unreconnected magnetosheath and magnetospheric field lines have been removed. Blue lines show magnetic field lines that have undergone reconnection; field lines are solid if they lie above the plane of the diagram, and dashed below it. Green lines mark the edge of the FTE. Estimating the cross sectional area of a flux rope from the FTE duration and velocity (circular in Figures 1a and 1b), and using that to calculate the flux content will provide an accurate estimate of the total flux transfer in Figure 1a; whereas in Figure 1b, this approach will only estimate the flux that maps through the flux rope:

$$\Phi_{\text{rope}} = B_{\text{axial}} \times \pi \times r^2 \tag{1}$$

As noted by Fear et al. (2008), this constitutes a minority of the flux opened by this burst of reconnection and a minority of the flux that maps to the ionospheric signatures. For the purposes of this paper, and in order to take a consistent approach between the spacecraft and ionospheric observations, we make an important distinction between the "flux transfer event" and the flux rope; we take the former to refer to the entire event—that is, the total flux that is opened by the burst of reconnection. In the Russell and Elphic (1978) model (Figure 1a), this is the same as the flux content of the flux tube; in the multiple X line model (Figure 1b), the flux that maps through the flux rope is a minority of the total flux, but the observation of a flux rope indicates the presence of much more significant opening of flux than is directly observed by the spacecraft. In the case of the single X line mechanism (Figure 1c), the resulting FTE structure is not a flux rope at all, and so it is inaccurate to assume so.

There is now plentiful evidence for the occurrence of FTEs caused by multiple X line reconnection: converging jets, consistent with multiple X lines, are observed (Hasegawa et al., 2010; Øieroset et al., 2011; Trenchi et al., 2011); there appears to be a seasonal control of the location at which in situ FTE signatures are observed (Korotova et al., 2008; Fear, Palmroth, & Milan, 2012) that is predicted by simulations (Raeder, 2006). Furthermore, the above mentioned reconstruction methods produce structures that appear consistent with the multiple X line mechanism (Hasegawa et al., 2006; Sonnerup et al., 2004). However, other studies report features more consistent with the single X line mechanism, for example, the observed evolution of the ion distribution

(Hwang et al., 2016; Lockwood & Hapgood, 1998), FTE velocities (Fear et al., 2007; Lockwood & Hapgood, 1998), and the presence of jets on the trailing edge of FTEs as a spatial feature (Trenchi et al., 2016). These two sets of observations need not be seen as contradictory — Trenchi et al. (2016) argued that it may be that both single and multiple X line mechanisms give rise to the observed in situ signatures, perhaps observed even on the same magnetopause crossings. Fear, Milan, and Oksavik (2012) compared a series of approaches to determine the axial orientation of flux transfer events observed on a magnetopause crossing where the magnetic shear across the magnetopause was close to 180° and concluded that the resulting axes were consistent with either of the long X line mechanisms, but not the original Russell and Elphic (1978) picture. On the other hand, Varsani et al. (2014) recently analyzed high cadence Cluster plasma data during the passage of an FTE and concluded the Russell and Elphic (1978) interpretation best described the observations. Higher-resolution plasma measurements, of the type now available from Magnetospheric Multiscale, are now revealing the detailed structure of flux transfer events (Eastwood et al., 2016; Farrugia et al., 2016; Hasegawa et al., 2016; Hwang et al., 2016; Zhao et al., 2016). However, in this paper, we outline a method to determine a more realistic value of the total FTE flux content that only requires the assumption that the observational signatures arise as a result of one of the longer X line mechanisms; for the purposes of this method, determination of the single versus multiple X line scenario is not required.

In the case of the multiple X line mechanism, the total flux transfer that occurs due to the burst of reconnection that gives rise to the flux rope in Figure 1b is given by the product of (a) the magnetopause area threaded by the open field lines that cross the magnetopause above (or below) the flux rope and that were opened during the formation of the flux rope, and (b) the B_N component across that area. Both of these quantities are difficult to measure directly. However, by symmetry, the resulting flux is equal to the flux that passes through the rectangle in Figure 1b, which is simply the product of the component of the magnetic field normal to the magnetopause (B_N) within the FTE, the radius of the flux rope (r), and the length of the flux rope (L):

$$\Phi_{\text{tot}} = B_N \times r \times L \tag{2}$$

Similarly, if the Southwood et al. (1988)/Scholer (1988) mechanism occurs, then the flux transferred is that which threads through the rectangle in Figure 1c, which is also given by equation (2). In both cases, the B_N component is that measured as the FTE passes the spacecraft and is therefore straightforward to deduce. Similarly, the FTE radius r is straightforward to calculate if the velocity and duration of the FTE structure are known. The only parameter that is difficult to deduce from spacecraft observations alone is the length of the FTE, L. Global-scale auroral observations and in situ observations from spacecraft at very large separations indicate that magnetopause reconnection can occur simultaneously at widely separated local times both in quasi-steady state (Phan et al., 2000) and as FTEs (Dunlop, Zhang, Bogdanova, Trattner, et al., 2011; Fear et al., 2009; Marchaudon et al., 2005; Milan et al., 2000). In this study, we adopt a similar approach and use spatially separated spacecraft and ionospheric observations to constraint the longitudinal extent of the FTEs we examine.

3. Instrumentation

In this study, we present observations from two intervals when we were able to monitor the dynamics of the magnetosphere using complementary in situ observations and global-scale observations of the ionospheric flow patterns. In situ measurements are provided by the four-spacecraft Cluster mission. We use 5 Hz magnetic field data from the fluxgate magnetometer on the Cluster 3 spacecraft (Balogh et al., 2001; Gloag et al., 2010) to investigate the in situ signatures of flux transfer events and calculate their flux content. In both intervals discussed, the Cluster spacecraft were situated at the dayside magnetopause at high latitudes in the Northern Hemisphere.

Information on the global-scale convection pattern, and ionospheric estimates of flux transfer, are derived from data from SuperDARN (Super Dual Auroral Radar Network) (Chisham et al., 2007; Greenwald et al., 1995). SuperDARN is a network of high-frequency radars that is designed to use backscatter from high-latitude field-aligned irregularities to trace the bulk plasma motion arising from large-scale magnetosphere-ionosphere coupling. Each radar transmits high-frequency radio waves, which are scattered from ionospheric density irregularities. When backscatter is detected, the line-of-sight velocity of the ionospheric plasma, backscatter power, and spectral width are measured. Data with a low velocity and low spectral width

are flagged as ground scatter. Each radar performs a full sweep of its field of view in 2 min. (For further details, see Milan et al., 1997.) In this paper, we present SuperDARN data from two individual radars (Prince George (PGR), situated in British Columbia, Canada, and Goose Bay (GBR) in Labrador, Canada), but we also combine data from multiple radars using the map potential technique (Ruohoniemi & Baker, 1998). This technique combines data from all available radars with data from a statistical model (to constrain the fitting process in regions with no data), in order to calculate the distribution of the ionospheric electrostatic potential as an expansion of spherical harmonics. In this way, an approximation of the global two-dimensional flow pattern can be derived.

Supporting observations of the solar wind are provided from the OMNI high-resolution data set (King & Papitashvili, 2005). During the intervals presented here, the data on which OMNI is based were provided by the magnetometer and plasma instruments on board the ACE spacecraft (McComas et al., 1998; Smith et al., 1998).

4. Observations and Results

In this section we outline our observations from two intervals. In the first, the Cluster spacecraft is separated from the cusp throat (as observed by SuperDARN) by several hours of local time, providing a good indicator of the minimum extent of the reconnection line. In the second, Cluster is closer to the cusp throat, reducing the information available on X line length but allowing us to investigate the one-to-one link between spacecraft and ionospheric signatures of flux transfer events.

4.1. Event 1: 8 February 2002

The first interval of interest is from 17:20 to 18:20 UT on 8 February 2002. The OMNI lagged solar wind conditions from 16:00 to 19:00 UT are shown in Figure 2. From 16:00 until 18:00 UT, the IMF was predominantly southward with a strong duskward component (a clock angle [arctan(B_Y/B_Z)] of ~90°). Then, from 18:00 to ~19:00 UT, the IMF gradually rotated northward, followed by a reversal in the B_Y component. The solar wind speed was steady at ~520 km s^{-1}, and the solar wind dynamic pressure was reasonably steady at ~1.5 nPa, with occasional increases to ~2 nPa due to modest increases in the proton density (density not shown).

The global-scale observations are summarized in Figure 3, which shows the ionospheric flow pattern observed at 17:50 UT plotted on a magnetic local time/magnetic latitude grid (with noon magnetic local time (MLT) at the top). The colored vectors represent fitted flow vectors derived from the map potential analysis method discussed in section 3. A twin cell convection pattern is evident, consistent with the driving of magnetospheric dynamics by a southward directed interplanetary magnetic field (Dungey, 1961). Antisunward flows are observed both in the prenoon sector (~8–10 MLT) and postnoon (~15–16 MLT), at latitudes of ~75–80°N. In the prenoon sector, the fast antisunward flows are also observed deeper into the polar cap; these flows are observed by the Prince George radar (PGR).

Due to lack of scatter, a data gap exists between ~10 and 13 MLT. At this time, the Cluster spacecraft were situated in the magnetosheath, near the high-latitude Northern Hemisphere magnetopause at $(5.6, 2.4, 10.0)_{GSM}$ R_E; however, the spacecraft were close enough to the expected location of the magnetopause that the Tsyganenko (1996) model parameterized for the conditions at the time (P_{dyn} = 1.6 nPa, Dst = −26 nT, IMF B_Y = 4.5 nT, and B_Z = 0) places the spacecraft on magnetospheric field lines. Therefore, the ionospheric footprint of Cluster 3 has been determined by tracing the location of the spacecraft down these model field lines to the ionosphere and is indicated by a red dot near noon (12.8 MLT, 76.7° MLAT). The location of the Cluster spacecraft therefore maps to the region in which there is a lack of scatter.

The observations made by Cluster (postnoon) and the Prince George radar (prenoon) between 17:20 and 18:20 UT are summarized in Figure 4. Figure 4 (first and second panels) shows time series of the B_N component and magnitude of the magnetosheath magnetic field observed by Cluster 3. (The magnetopause normal, $(0.749, 0.355, 0.559)_{GSE}$ is determined from the Shue et al., 1998 model.) A series of clear bipolar variations in B_N are observed, indicative of northward moving FTE signatures, coupled with enhancements in the magnetic field strength. Figure 4 (third and fourth panels) shows the backscatter power and line-of-sight velocity observed in Beam 10 of PGR, plotted against magnetic latitude and time. (The orientation of Beam 10 is indicated by a dashed blue line in Figure 3.) A series of radar poleward moving auroral forms (PMAFs) is evident, which are the characteristic radar signatures of FTEs. These patches typically propagate from a magnetic latitude of ~75° to ~82°N MLAT before a new PMAF forms at ~75°. The line-of-sight velocities corresponding to these PMAFs are typically greater than 800 m s^{-1} and directed away from the radar (poleward).

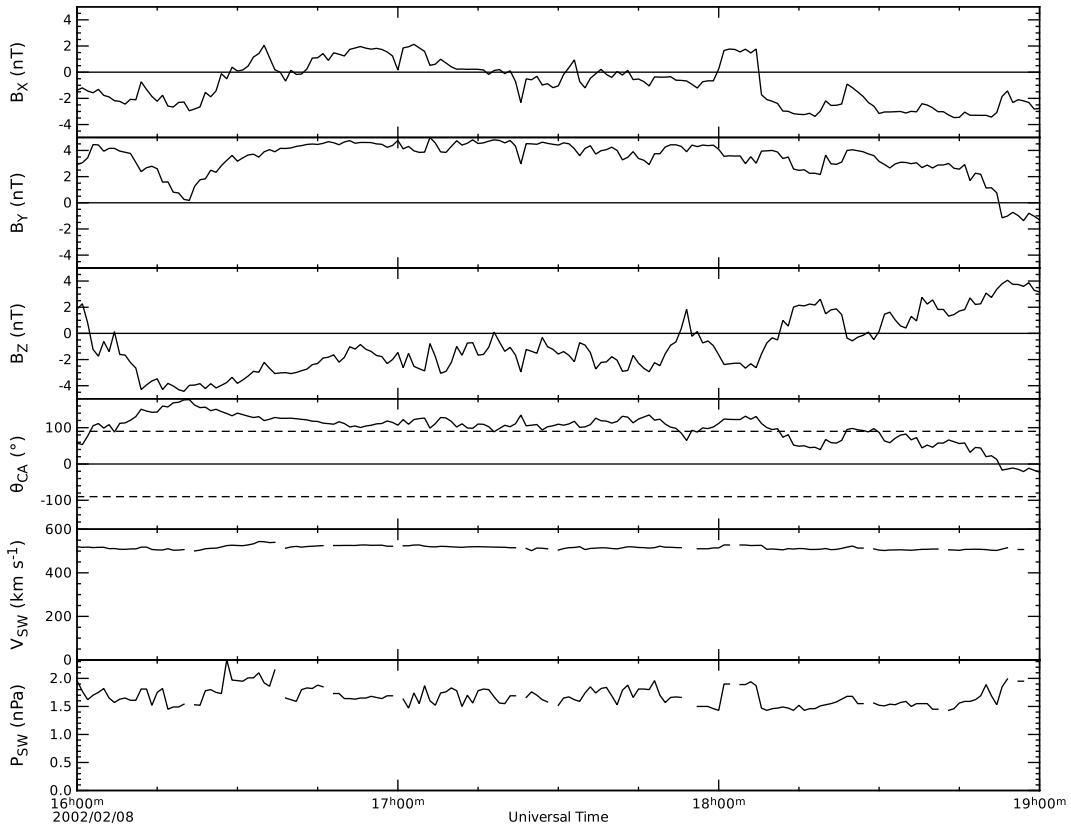

Figure 2. Solar wind conditions from 8 February 2002. (top to bottom) The GSM components of the interplanetary magnetic field, the IMF clock angle (dashed lines indicate ±90°), and the solar wind speed and dynamic pressure.

Milan et al. (2000) calculated the area opened by each burst of reconnection by multiplying the poleward distance along which the radar PMAFs were observed to propagate by the estimated extent of the merging gap (the ionospheric projection of the reconnection line). They estimated that each FTE signature was observed to expand 500 km poleward into the polar cap and to extend 3,000 km along the polar cap boundary. In our case, the PMAFs observed in Figure 4 are observed to propagate by ~7° of magnetic latitude into the polar cap, corresponding to a poleward propagation of 700 km. We estimate the extent of the reconnection line from Figure 3. Although there is a gap in the SuperDARN backscatter in the noon sector, we take the observation of in situ signatures by Cluster as clear evidence that bursty reconnection is taking place in this sector too. Although it is difficult to identify a 1:1 correlation between the FTE signatures observed by Cluster and those observed by PGR, there appear to be a similar number of FTE signatures in the two data sets during this 1 h interval. (In Figure 4 we identify 10 clear FTE signatures observed by Cluster, each of which are identified by a clear, isolated B_N signature and most of which are accompanied by an enhancement in |B|, and seven clear PMAFs.) We therefore proceed on the assumption that the reconnection bursts are occurring coherently between PGR and Cluster, though we will return to discuss the validity of this assumption in section 4.2.

If we take the length of the merging gap (indicated by a pink dashed line in Figure 3) to be the distance from the westward edge of the PMAFs observed by PGR (at 7 MLT), along the 76.7°N MLAT contour, to the footprint of the Cluster spacecraft, that corresponds to a length of 2,200 km (5.8 h of MLT). Therefore, an area of 1.5×10^6 km^2 is opened in each burst of reconnection, corresponding to an opening of 77 MWb per event (which we call Φ_{SD}). This is comparable to the estimate made by Milan et al. (2000) (see Table 1). If we take the uncertainties in the MLT extent to be ±1 h and in the latitudinal extent of the expansion to be ±2°, this leads to a uncertainty on Φ_{SD} of ±26 MWb.

Our estimate of Φ_{SD} can be compared with different estimates of the flux transfer from the spacecraft observations (Φ_{rope} and Φ_{tot}) from equations (1) and (2) above. The FTE observed at 17:59 UT (third vertical arrow from right in Figure 4) was observed by all four Cluster spacecraft (not shown); and therefore, its speed was determined from multispacecraft timing analysis (Harvey, 1998) as 160 km s^{-1}. The passage of the FTE lasted

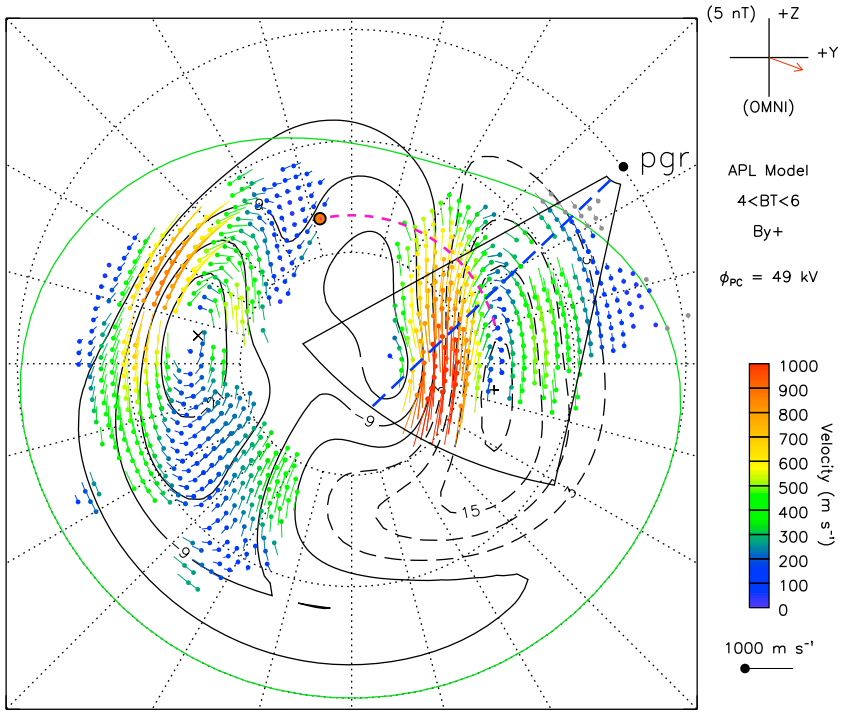

Figure 3. Global ionospheric flow pattern at 17:50 UT on 8 February 2002, derived from SuperDARN observations using the map potential analysis technique (Ruohoniemi & Baker, 1998). Vectors are plotted on a magnetic local time/magnetic latitude grid, with noon MLT at the top and dawn to the right. Local time and latitude contours are shown at 1 h/10° intervals. The field of view of the Prince George radar (PGR) and the footprint of the Cluster spacecraft (red dot) are shown. The dashed blue line in the PGR field of view indicates the direction of Beam 10, and the dashed pink line indicates the ionospheric projection of the assumed reconnection line used for flux calculations.

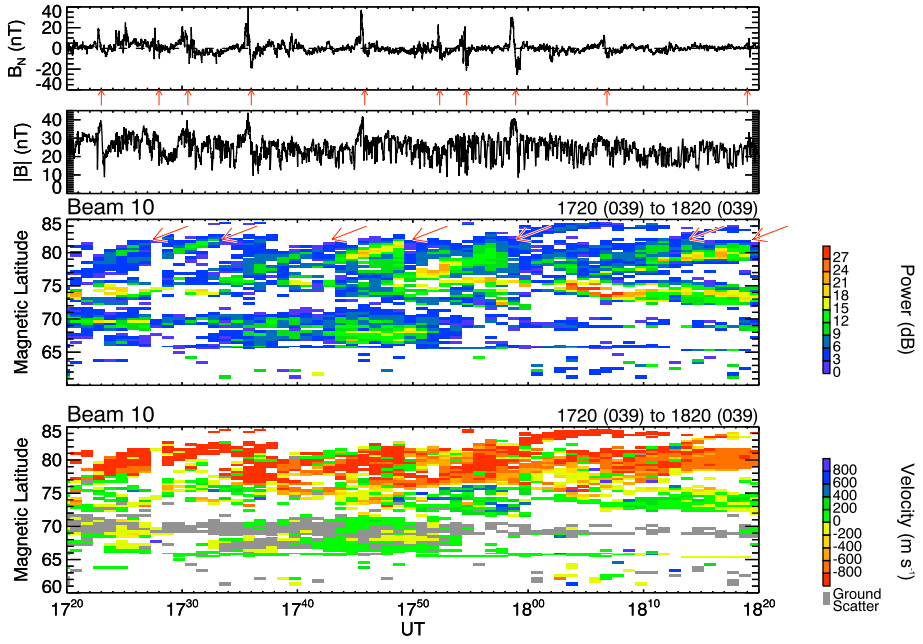

Figure 4. Time series of the observations of flux transfer events made by Cluster 3 and the Prince George radar. (first and second panels) The B_N component and magnitude of the magnetosheath magnetic field observed by Cluster 3. (third and fourth panels) The backscatter power and line-of-sight velocity observed in Beam 10 of the Prince George radar.

approximately 60 s, resulting in an estimate of the radius of 4,800 km. The FTE duration is toward the higher end, and the velocity and radius toward the lower end of the typically observed range (Fear et al., 2007, Figure 6), but none of these three values are outliers. The peak value of |B| during the passage of each FTE in Figure 4 is 40 nT, which we take to be representative of the axial field component at the center of the FTE. Substituting these values into equation (1) leads to a value of Φ_{rope} of 3 MWb (typical of the spacecraft values in Table 1). Estimating the uncertainty in this value is a little trickier, as the main source of error will be the fact that the spacecraft may not have crossed the center of the FTE; therefore, B_{axial} may have been underestimated. We therefore assume that B_{axial} may potentially be 50% greater and take the uncertainty on this value to be $\pm$20 nT. We assume that the speed and hence r are relatively well defined with an uncertainty of $\pm$10%. This results in an uncertainty on Φ_{rope} of $\pm$1.5 MWb, which is large in relative terms but clearly not large enough to explain the mismatch between Φ_{rope} and Φ_{SD}.

In order to estimate Φ_{tot} from equation (2), we need an estimate of the length of the reconnection line at the magnetopause, L. To do so, we trace along the Shue et al. (1998) model magnetopause from the location of Cluster to the point where a Tsyganenko (1996) field line trace results in a footprint matching the westward edge of the PMAFs (the westward edge of the pink dashed line) in Figure 3; this results in an X line length of 240,000 km (38 R_E). Strictly speaking, the value of B_N in equation (2) is that observed during a crossing when the spacecraft crosses through the center of the FTE (perfectly tangential to the surrounding magnetopause surface). In order to obtain a realistic value, we use the peak value of B_N observed in Figure 4 (40 nT) and assume the same relative uncertainty of $\pm$50%, which results in an estimate of Φ_{tot} of 46$\pm$25 MWb. We note in passing that the uncertainty associated with B_N is more likely to lead to an underestimate of the total flux, as the observed peak value of B_N is likely to be an underestimate of the true peak value given the idealized crossing described above; however, the radius estimate is likely to contribute to an overestimate of flux as it is determined from the duration of the magnetic signature, which is in part due to the draping of field lines around the open FTE "core." Therefore, overall, the error bars can be taken to be symmetric. The error bars on Φ_{tot} and Φ_{SD} overlap, and hence, these two values agree within their (relatively large) uncertainties.

The two major factors that are not incorporated into the uncertainty measurements in this section are the two related assumptions that (i) the reconnection process occurs coherently across the 6 h of MLT between the spacecraft and the cusp throat, and (ii) that the link between the spacecraft and ionospheric signatures is one to one (which is not quite the case in Event 1, perhaps due to the separation in local time). We now seek to investigate the validity of these two assumptions. The ratio between Φ_{tot} and Φ_{SD} in Event 1 is actually not very sensitive to the precise choice of reconnection line length, as a larger merging gap inferred from Figure 3 leads to a (nearly) proportionately larger X line length mapped out at the model magnetopause. (The Tsyganenko 1996 model magnetic field lines are not strictly contained in meridional planes, but instead flare out, leading to small changes in the ratio of the two values.) For example, poleward flows are observed at 14–16 MLT in Figure 3, though there are no clearly distinct pulsed PMAF signatures; if the ionospheric merging gap is taken to extend to this sector (9 h in MLT or 2,600 km), then the corresponding X line length at the magnetopause is 50 R_E and the values of Φ_{tot} and Φ_{SD} are 58 MWb and 91 MWb—the ratio Φ_{tot}/Φ_{SD} is 64% as opposed to 60%. (The value of Φ_{rope} does not depend on the X line length.) Therefore, in order to investigate the assumptions of coherence and the one-to-one link between signatures, in the following subsection we examine a complementary event where the footprint of the Cluster spacecraft is much closer to the cusp throat. Although we therefore lose information about the total spatial extent of the X line (and therefore the total flux transfer), we can still compare the ratios of Φ_{tot} to Φ_{SD} with more confidence that the assumptions made are valid.

4.2. Event 2: 11 March 2006

The period selected for our second case study is from 14:00 to 14:30 UT on 11 March 2006. The solar wind conditions from 12:00 to 16:00 UT are shown in Figure 5. During this period, the IMF was northward, but at times the IMF B_Y component was strong; the clock angle therefore alternated between periods where it was close to zero and periods close to +90°. The solar wind speed was steady at ~550 km s^{-1}; the solar wind dynamic pressure varied between 2.5 and 3.5 nPa as a result in small variations in the solar wind density (density not shown).

The global-scale observations for this event are summarized in Figure 6, in the same format as Figure 3. This time, there is considerably less scatter globally, though there is a good level of scatter local to the Goose Bay (GBR) radar where there is evidence of antisunward flows at this time. These flows are indicative of dayside

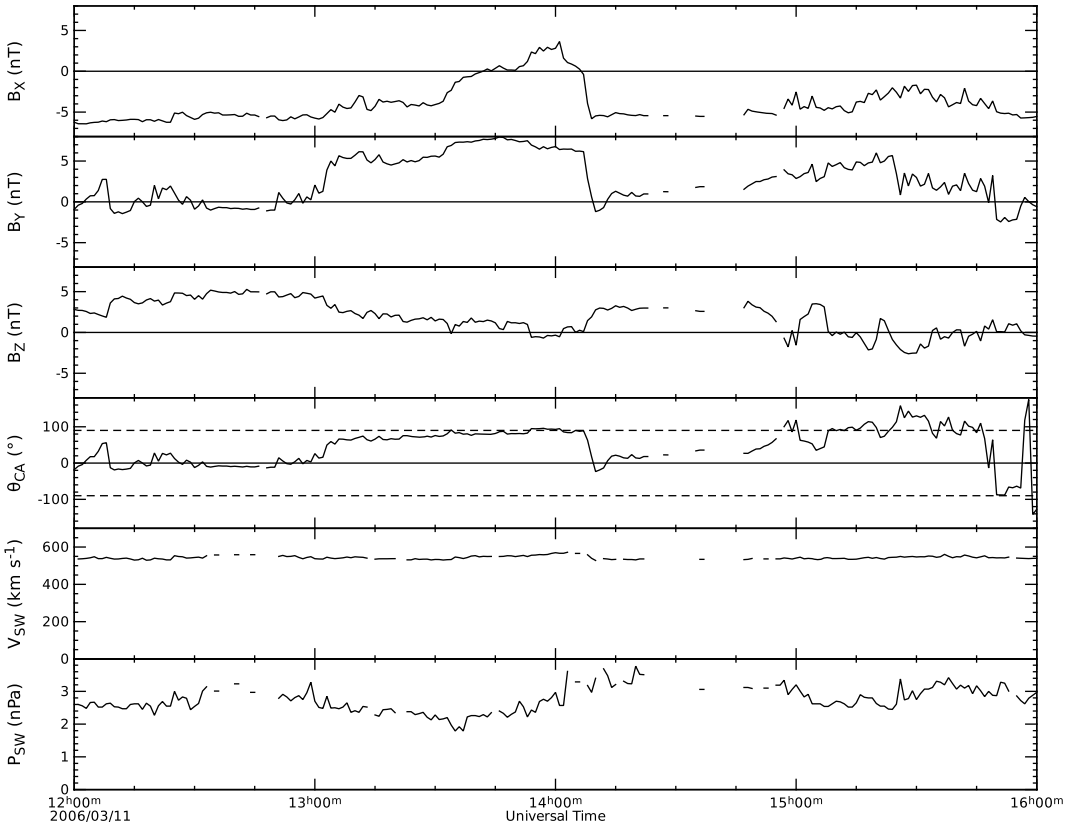

Figure 5. Solar wind conditions from 11 March 2006 in the same format as Figure 2.

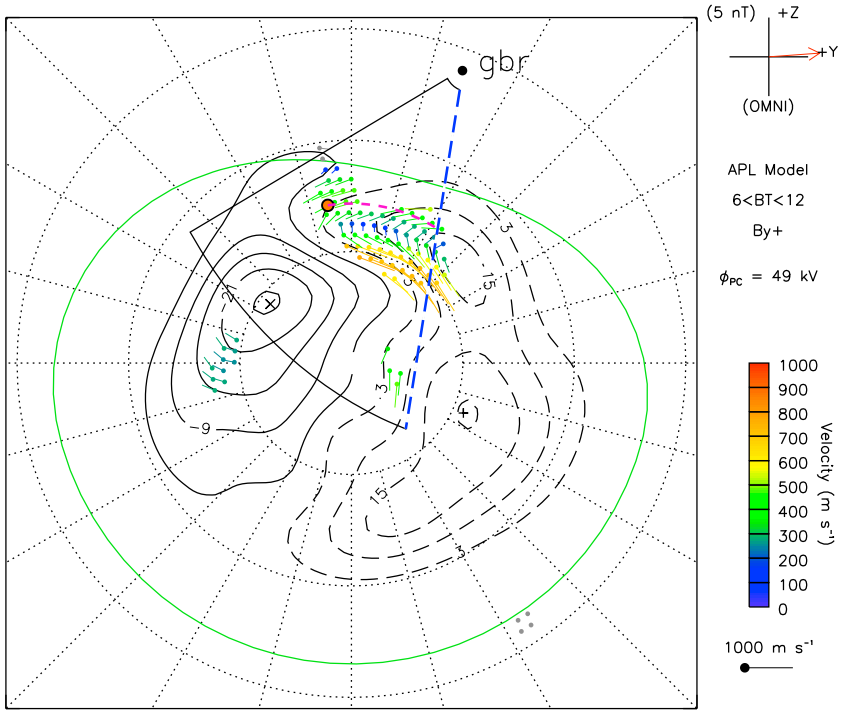

Figure 6. Global ionospheric flow pattern at 14:00 UT on 11 March 2006 (in the same format as Figure 3). The field of view of the Goose Bay radar (GBR) and the footprint of the Cluster spacecraft (red dot) are shown. Time series data shown in Figure 7 are taken from Beam 0, which is along the dawnward side of the field of view (blue dashed line). The pink dashed line indicates the ionospheric projection of the reconnection line assumed for flux calculations.

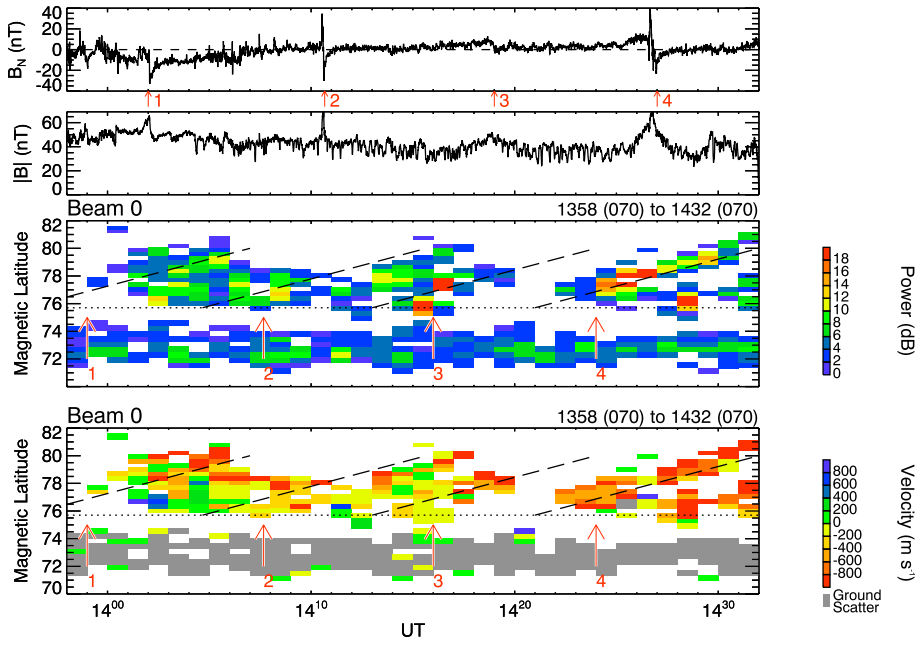

Figure 7. Time series of the observations of flux transfer events made by Cluster 3 and the Goose Bay radar on 11th March 2006. Top two panels: the B_N component and magnitude of the magnetosheath magnetic field observed by Cluster 3. Bottom two panels: the backscatter power and the line-of-sight velocity observed in Beam 0 of the Goose Bay radar. The guidelines in the bottom two panels are initially plotted for PMAF 4 (based on the backscatter power), and then offset to the left by the respective offsets of times of observation of FTEs 1, 2 and 3 by Cluster 3 (relative to FTE 4).

reconnection taking place, which is consistent with the fact that the IMF clock angle is close to 90° at this time (e.g., Trattner et al., 2017, and references therein). At this time, the Cluster tetrahedron straddled the magnetopause; the Tsyganenko (1996) model, parameterized by the conditions at 14:00 UT (P_{dyn} = 3.0 nPa, $Dst = -10$ nT, IMF B_Y = 6 nT, and B_Z = 0), places the footprint of the Cluster spacecraft at the eastward edge of the observed backscatter, again indicated by a red dot (12.6 MLT, 75.7° MLAT). The location of the Cluster footprint is close to the latitude at which the flows reverse in a manner consistent with newly opened field lines entering the polar cap.

The observations made by Cluster 3 (at 12.6 MLT) and Beam 0 of the Goose Bay radar (9.9 MLT at the open-closed field line boundary, taken to be the magnetic latitude of the Cluster footprint) are summarized in Figure 7, in the same format as Figure 4. In Figure 7 (first panel), the magnetopause normal of $(0.936, 0.128, 0.329)_{GSE}$ has again been determined from the Shue et al. (1998) model. Four clear bipolar B_N signatures (labeled with red arrows) are accompanied by enhancements in |B|. In addition, before 14:00 UT there are a couple of candidate bipolar signatures (one of which may be associated with an enhancement in |B|, but neither of which correspond to any significant ionospheric backscatter), and between 14:05 and 14:09 UT there is a rapid sequence of B_N variations (though not clearly correlated with |B| behavior). Therefore, the four highlighted events are identified for further examination based on the fact that they occur after 14:00 UT (and hence correspond to observed ionospheric backscatter) and exhibit a clear |B| enhancement.

At first sight, Figure 7 (third panel) (which shows backscatter power) appears to show evidence for three poleward moving radar auroral forms, centered on ~14:04, 14:14, and 14:27 UT. Of these, the clearest is the final PMAF, which can be seen clearly to propagate from 77° to 81° MLAT. In order to further investigate the relationship between the observed in situ and ionospheric signatures of FTEs in this interval, we have added a dashed guide line to show the poleward expansion of PMAF 4 (which we take to correspond to the in situ signature of FTE 4) and reproduced the same line three times, offset to the left by the respective offsets of times of observation of FTEs 1, 2, and 3 by Cluster 3 (relative to FTE 4). The results are revealing: the lefthand-most guideline lines up neatly with the first PMAF (as viewed in the backscatter power); the second and third guidelines line up with different parts of the backscatter that we had previously interpreted as a single PMAF. The guideline corresponding to FTE 2 lines up with an enhancement of backscatter power at 76–78° MLAT between 14:06 and 14:09 UT, and the same guideline lies just poleward of a patch of enhanced backscatter

power at 77–80° MLAT between 14:11 and 14:18 UT. The guideline corresponding to FTE 3 then aligns with a patch of enhanced backscatter power that can be observed to propagate poleward from 76° MLAT, starting at 14:14 UT. We therefore suggest that the initial stages of the PMAF corresponding to FTE 2 are observed by the GBR radar, and either this PMAF propagates more slowly than the others (indicating a lower reconnection rate but accumulating to the same total amount of flux opened as in the other events) or GBR observes the later stages of an additional PMAF that does not exhibit a corresponding in situ signature at Cluster. Then the initial stages of the PMAF corresponding to FTE 3 are observed by GBR, but the backscatter fades in its later stages. All four guidelines are also overlaid in Figure 7 (fourth panel; backscatter velocity), which shows that the four PMAF signatures are associated with fast negative flows that correspond to flows away from the radar.

Therefore, in this second case study, there is much clearer evidence for a one-to-one correlation between the FTE signatures observed by Cluster and the corresponding PMAF signatures observed by SuperDARN. We repeat the calculations carried out in section 4.1. The separation between the footprint of the Cluster and the intersection of Beam 0 at the open/closed field line boundary (again taken to be the magnetic latitude of the Cluster footprint) is 2.7 h of MLT, which corresponds to a merging gap length in the ionosphere of 1,000 km (pink dashed line in Figure 6). The PMAFs are observed to expand poleward by 4°, from 77° to 81° N MLAT, which corresponds to a poleward distance of 400 km. Therefore, the area of polar cap opened by each FTE is 4×10^5 km^2. This time, since we are estimating the flux opened in the specific sector marked in Figure 6, not the total flux opened, we take the estimate of the merging gap length to be exact (since this will also feed into the calculation of Φ_{tot}) but again assume that the uncertainty on the magnetic latitude extent of the PMAFs is ±2°. This gives rise to an estimate of Φ_{SD} of 20±10 MWb. From multispacecraft measurements (not shown) of the largest and clearest in situ signature, FTE 4, we infer its speed of propagation to be 340 km s^{-1}; the passage of the FTE lasts approximately 38 s, which implies a radius of 6,500 km. All three values are close to the median values for FTEs observed by Cluster (Fear et al., 2007). We again take B_{axial} to be the peak value of |B| observed during this interval (70 nT); applying the same assumptions about uncertainties as in section 4.1 results in an estimate of Φ_{rope} of 9 ± 5 MWb. Tracing from the location of Cluster, along the Shue et al. (1998) model magnetopause, to a location where the Tsyganenko (1996) model footprint is at the same MLT as the western end of the pink dashed line in Figure 6 results in an estimate of the X line length (L) of 61,000 km (9.5 R_E), which corresponds to the merging gap used to calculate Φ_{SD}. Again, taking the peak value of B_N (40 nT) and assuming the X line length is exact (for comparison with Φ_{SD}), but making the same assumptions about the uncertainties in B_N and r as in section 4.1 leads to an estimate of Φ_{total} of 16 ± 8 MWb. The estimates of Φ_{SD} and Φ_{total} match extremely well, though all three flux values agree within their error bars.

5. Discussion

The flux estimates derived in section 4 are summarized in Table 2, and the values of Φ_{SD} and Φ_{tot} for Event 1 (8 February 2002) are included in Table 1. In the case of Event 1, there is a major difference between the flux calculated based on the flux rope (Φ_{rope}, equation (1)) and the flux estimated from the SuperDARN observations (Φ_{SD}), but our proposed means of calculating the flux from in situ measurements (Φ_{tot}, equation (2)) agree with Φ_{SD} within the somewhat large error bars. As discussed in section 4.1, two major factors are not incorporated into these error bars — the assumptions that (i) reconnection occurs coherently over the 6 h of MLT between the spacecraft and the cusp throat, and (ii) that the link between the spacecraft and ionospheric signatures is one to one. Neudegg et al. (2000) found a majority of in situ FTE signatures, or groups of FTE signatures, were associated with ionospheric flow signatures, and vice versa; however, a significant minority of events were not associated with a corresponding signature, and Neudegg et al. (2000) also found it necessary to group in situ signatures, making a one-to-one link less clear in their statistical study. However, in a group of illustrative case studies, they identified that when the inter-FTE spacing (observed in situ) was greater than ~5 min, then clearly spaced ionospheric flow signatures could generally be identified, and the ionospheric flow velocity tended to return to a baseline level afterward. On the other hand, when the inter-FTE spacing was less than ~5 min, the response functions for individual events tended to convolve. In the case of Event 1, at least 10 in situ FTE signatures were observed by Cluster in a 60 min interval, and the inter-FTE period was sometimes as low as 2 min. Even neglecting assumption (i), the results of Neudegg et al. (2000) suggest we would not expect to clearly identify individual ionospheric response signatures to specific in situ FTEs. On the other hand, during Event 2, the interplanetary conditions were more conducive to a lower reconnection rate (the IMF clock angle was generally lower), the inter-FTE spacing observed by Cluster was also larger (4 FTEs separated by 8–9 min each), and a clearer one-to-one link with the ionospheric signatures was observed (aided also by the fact that

Table 2
Flux Estimates (Per FTE) From This Study

Event	Date and time	No. of FTEs	Φ_{SD}	Φ_{rope}	Φ_{total}
1	8 February 2002 17:20–18:20 UT	7–10	77 ± 26 MWb	3 ± 1.5 MWb	46 ± 25 MWb
2	11 March 2006 14:00–14:30 UT	4	20 ± 10 MWb[a]	9 ± 5 MWb	16 ± 8 MWb[a]

[a]Estimate of flux opened between 9.9 and 12.6 MLT only.

the Cluster footprint was closer to the cusp throat, and hence variations in reconnection rate along the length of the reconnection line can be expected to be less significant). In the case of the second event the estimates of Φ_{SD} and Φ_{total} are much closer, giving us confidence that the method outlined in equation (2) is reliable means of estimating the flux transferred by FTEs from in situ measurements (plus an estimate of the reconnection line length, which can realistically usually only be determined from ionospheric measurements). This method can therefore resolve the discrepancy between spacecraft and ionospheric measurements discussed in section 1 and Table 1. The implication is that past estimates of FTE flux transfer determined from ionospheric measurements are more representative of the total flux transfer by FTEs (as opposed to the subset of flux that maps through the flux rope, in the case of the Lee and Fu (1985) mechanism). This in turn suggests that FTEs, and hence bursty reconnection, may be the dominant mode of driving the terrestrial magnetosphere.

The ionospheric flux estimates made in this study and by Milan et al. (2000) are the largest estimates in Table 1. The upper end of the range reported by Lockwood et al. (1990) is of the same order of magnitude (approximately half those inferred from Milan et al., 2000 and calculated here), but several other studies (Marchaudon, Cerisier, Greenwald, et al., 2004; Marchaudon, Cerisier, Bosqued, et al., 2004; Oksavik et al., 2005) report smaller values that are comparable to the spacecraft estimates in Table 1. This is primarily as a result of a much lower assumed or observed extent of the ionospheric projection of the reconnection line; the poleward extents of propagation of the PMAFs reported in this study (Event 1) and by Milan et al. (2000) are ∼7° and ∼5°, respectively, which both lie above (but close to) the center of the statistical distribution reported by Provan and Yeoman (1999) (their Figure 5a). Similarly, the inferred MLT extent of the reconnection site, though inferred here from separate SuperDARN and Cluster observations, is also above (but close to) the center of the statistical distribution of the MLT extents of pulsed ionospheric flows reported in Figure 9 of Provan and Yeoman (1999). It is also comparable to the extent of the magnetopause reconnection line inferred by Wild et al. (2003) from their interpretation of the observed ionospheric flow pattern in conjunction with Cluster in situ observations. Therefore, the events reported here (Event 1) and by Milan et al. (2000) are large, but not extreme, in terms of their extent and hence flux transfer.

In the case of Event 2, we note that the calculated value of Φ_{rope} is also consistent with Φ_{SD} and Φ_{total} within the error bars (which is not the case for Event 1). The expression for Φ_{rope} does not depend on the length of the reconnection line (equation (1)), and so in cases where the X line length can be shown to be short (or, as is the case in Event 2, where limited scatter means we cannot be sure of the overall extent of the reconnection line and so the flux transferred is only evaluated over a local part of the magnetopause), the tacit assumption that the FTE structure is that proposed by Russell and Elphic (1978) results in a much less significant discrepancy. In other words, the discrepancy between ionospheric and in situ flux estimates only becomes significant if the reconnection line is long enough. However, on the assumption that FTEs are, in fact, generated by either the single or multiple X line mechanisms, then we would argue that in the situation of a short X line (or X lines), the fact that the estimates for Φ_{rope} and Φ_{SD} match is not an indicator that Φ_{rope} is the strictly correct way to estimate the flux transferred by FTEs. In the case of the multiple X line mechanism (Figure 1b), the total flux transferred by an FTE strictly consists of the sum of Φ_{rope} and the value of Φ_{total} determined from equation (2); the ratio of these two components depends on the length of the X line, so for Φ_{rope} to be the major contributor to the total flux, the X line length must be less than the flux rope radius—in which case the second X line in Figure 1b barely has any influence. As noted in section 2, in the case of the single X line mechanism, the resulting structure is not a flux rope, and so evaluating Φ_{rope} is not strictly correct.

The major obstacle to evaluating the flux content of FTEs is the determination of the spatial extent of the FTE in the magnetopause plane, perpendicular to its direction of propagation. This is difficult with in situ measurements, even with multispacecraft observations, as the separation must be large enough to ensure that the same FTE is observed, without being too large to leave open the possibility that different events are observed.

Fear et al. (2008) and Fear et al. (2010) reported observations from seasons when the Cluster spacecraft crossed the magnetopause with a separation of order 10,000 km; in the former study, they found FTEs with a minimum azimuthal scale that was greater than their poleward extent, but in the latter study they found events that were spatially patchy, even on the spacecraft separation scale. Other studies have used conjunctions of different spacecraft missions and reported near-simultaneous observations of FTEs at very different magnetic local times (e.g., Dunlop, Zhang, Bogdanova, Trattner, et al., 2011; Dunlop, Zhang, Bogdanova, Lockwood, et al., 2011; Fear et al., 2009; Marchaudon et al., 2005), but in such cases it is difficult to show that reconnection occurs coherently between the local times at which the observations are made. Lockwood et al. (1995) circumvented this limitation by using the single X line mechanism and observed FTE statistics to determine the upper limit for FTE flux transfer. Based on these arguments, they found the upper limit for the voltage contribution of FTEs to be in the range 50–200 kV, which they found to be comparable with the average reconnection voltage for southward IMF, and hence concluded it was possible that FTEs could provide all of the dayside reconnection voltage. They noted that this upper limit, having been determined statistically, does not rely on the determination of the azimuthal extent of individual FTEs, as the upper limit could equivalently be contributed by individual FTEs spanning the entire azimuthal extent of the dayside magnetopause or by multiple shorter FTEs occurring simultaneously at different local times.

The Milan et al. (2000) study cited above presented the first FTE signatures in auroral images on a near-global scale taken from space. Recently, Milan et al. (2016) have presented the second such set of observations. The two sets of observations reported in these two papers occurred at similar times of year and for similar IMF conditions; however, the local time extent of the observed FTE signatures and the concurrent solar wind speed differed, as did the cross polar cap potential (inferred from SuperDARN data). Milan et al. (2016) speculated that the azimuthal extent of the FTE signatures (i.e., length of the X line) may depend on the solar wind speed; in the earlier study the FTEs spanned at least 7 h of MLT and the solar wind was high ($\sim$650 km s^{-1}), whereas in the latter study the auroral FTE signatures were narrower ($\sim$2 h of MLT) and the solar wind speed was lower ($\sim$450 km s^{-1}). The authors noted that empirical expressions for the global reconnection rate as a function of upstream conditions depend upon the solar wind speed (as well as IMF conditions), and that the FTEs occurring in the two intervals they studied did so at a similar rate ($\sim$ every 7–8 min); they therefore suggested that in the two cases studied, the different overall reconnection rate was achieved by different lengths of reconnection line. We agree with Milan et al. (2016) that a comprehensive study of the extent and variability of ionospheric reconnection signatures of reconnection is warranted, but in the meantime note that the solar wind speeds for our two events are similar ($\sim$520/540 km s^{-1}); however, the limited scatter available for Event 2 means we cannot be sure of the true extent of the reconnection line or FTE signatures for this event. The key difference between our selected events was in the IMF conditions (for Event 1, the IMF was duskward and southward, whereas for Event 2 it was duskward and slightly northward). The expected reduction in the global reconnection rate for Event 2 resulting from the less favorable IMF conditions appears to have been manifested as a reduction in the frequency of FTEs, such that individual ionospheric responses could be resolved (Neudegg et al., 2000), though the magnetic field strength in the center of the in situ signatures was greater, as was the "per event" value of Φ_{rope} (Table 2).

There are two areas in which our results have particular implication. The first is at Mercury, where several studies have reported proportionally larger flux contents (compared with the size of Mercury's polar cap) than those at Earth (e.g., Russell & Walker, 1985; Slavin et al., 2010). Imber et al. (2014) reported a statistical study of large-amplitude FTEs (where the peak |B| in the FTE exceeded the magnetic field strength just inside the magnetopause) and found a mean flux content of 0.06 MWb, including one event containing 0.22 MWb. Mercury's polar cap is believed to contain typically 4–6 MWb (Alexeev et al., 2010); a large (but not atypical) Hermean FTE may therefore open 1–2% of Mercury's polar cap and an extreme event may open 5%. Coupled with their high repetition rate (Slavin et al., 2012), FTEs are already believed to be the major driver of Mercury's magnetospheric dynamics (Imber et al., 2014); however, these flux estimates are also based on the tacit assumption of a Russell and Elphic (1978) flux rope, or neglecting the "additional" flux discussed by Fear et al. (2008) that is opened by the burst of reconnection, but does not map through the flux rope in the Lee and Fu (1985) model. These studies may therefore also underestimate the total contribution of FTEs to Mercury's dynamics. Since at Earth, including this additional flux can increase the flux estimate by a factor of 10 (Tables 1 and 2), a similar discrepancy at Mercury would imply that individual FTEs there might cause the polar cap area to increase by 50%. Whether this extreme is reached would depend upon whether typical conditions at Mercury make the discrepancy more akin to our Event 1 or Event 2; this is something we intend to investigate in a future study.

The other wider implication our work has is for flux closure in the magnetotail of Earth (and other planets). Slavin et al. (2003) presented a statistical study of earthward moving and tailward moving magnetotail flux ropes observed in the plasma sheet by Geotail at $X > -30\ R_E$ and included in their analysis the fitting of the force-free flux rope model to their observations. They found mean flux contents of 1.1 and 9.1 MWb for earthward moving and tailward moving flux ropes, respectively, corresponding to 0.2% and 2% of the flux content of the lobes (or polar cap), respectively. While these do indeed refer to the flux content of the flux ropes, the arguments discussed in this paper also apply when considering the total flux transport, and depending on the length of the reconnection lines in the magnetotail, the flux closed in the formation of these flux ropes may be significantly greater.

6. Conclusions

We have presented a simple new method to calculate the total flux transferred by flux transfer events, based on in situ observations supplemented by an estimate of the length of the flux transfer event/reconnection line (which can be inferred from ionospheric measurements). We argue that if flux transfer events are formed by either of the longer X line mechanisms (either from a single X line, Scholer, 1988; Southwood et al., 1988, or multiple X lines, Lee & Fu, 1985), this gives a more accurate estimate of the overall flux transfer per event than by calculating only the flux that maps through the flux rope itself. We have tested this method against two conjunctions between the Cluster spacecraft and the SuperDARN ionospheric radars. In the first event, the Cluster footprint was about 6 h of MLT duskward of the cusp throat; FTE signatures were observed by both Cluster (at the magnetopause) and SuperDARN (in the cusp throat). A similar number of reconnection signatures was observed, but the correlation was not quite one to one. Nonetheless, the total flux we calculated based on the in situ measurements was consistent (within error bars) with the flux estimate from SuperDARN observations, whereas the usual estimate (of flux mapping through the flux rope) was not. In a second event, the Cluster footprint was much closer to the cusp throat, the inter-FTE period was longer, and a one-to-one correlation between spacecraft and ionospheric signatures was observed. Although for this event we have incomplete information on the length of the X line (and hence FTEs), when calculated across the local MLT sector much of the remaining discrepancy was removed (though when considering a short X line, the effect of the tacit assumption made when equating flux rope content with total FTE content is much less significant). We therefore agree with Lockwood et al. (1995) and Milan et al. (2000) that flux transfer events may be the dominant means of driving the Dungey cycle at Earth. However, further work should be done on a wider event base, with a range of local time extents, to verify our conclusions.

Acknowledgments
R. C. F. was supported by the UK's Science and Technology Facilities Council (STFC) Ernest Rutherford Fellowship ST/K004298/2; L. T. and J. C. C. were supported by STFC Ernest Rutherford grant ST/L002809/1, and S. E. M. was supported by STFC consolidated grant ST/N000749/1. SuperDARN is a collection of radars funded by national scientific funding agencies of Australia, Canada, China, France, Japan, South Africa, United Kingdom, and the United States of America. Data were obtained from the British Antarctic Survey SuperDARN data hub and processed with RST v4.0 and FITACF v3.0. Cluster data were obtained from the Cluster Science Archive (https://www.cosmos.esa.int/web/csa). We are grateful to Paul Breen, Pasha Ponomarenko, Kevin Sterne, and Keith Kotyk for their assistance with the SuperDARN data hub, RST, and FITACF.

References

Alexeev, I. I., Belenkaya, E. S., Slavin, J. A., Korth, H., Anderson, B. J., Baker, D. N., … Solomon, S. C. (2010). Mercury's magnetospheric magnetic field after the first two MESSENGER flybys. *Icarus*, *209*, 23–39. https://doi.org/10.1016/j.icarus.2010.01.024

Amm, O., Donovan, E. F., Frey, H., Lester, M., Nakamura, R., Wild, J. A., … Strømme, A. (2005). Coordinated studies of the geospace environment using Cluster, satellite and ground-based data: An interim review. *Annales Geophysicae*, *23*, 2129–2170. https://doi.org/10.5194/angeo-23-2129-2005

Balogh, A., Carr, C. M., Acuña, M. H., Dunlop, M. W., Beek, T. J., Brown, P., … Schwingenschuh, K. (2001). The Cluster magnetic field investigation: Overview of in-flight performance and initial results. *Annales Geophysicae*, *19*, 1207–1217. https://doi.org/10.5194/angeo-19-1207-2001

Browett, S. D., Fear, R. C., Grocott, A., & Milan, S. E. (2017). Timescales for the penetration of IMF B_Y into the Earth's magnetotail. *Journal of Geophysical Research: Space Physics*, *122*, 579–593. https://doi.org/10.1002/2016JA023198

Chisham, G., Lester, M., Milan, S. E., Freeman, M. P., Bristow, W. A., Grocott, A., … Walker, A. D. M. (2007). A decade of the Super Dual Auroral Radar Network (SuperDARN): Scientific achievements, new techniques and future directions. *Surveys in Geophysics*, *28*, 33–109. https://doi.org/10.1007/s10712-007-9017-8

Cowley, S. W. H. (1981). Magnetospheric and ionospheric flow and the interplanetary magnetic field. In *Physical basis of the Ionosphere in the Solar-Terrestrial System* (pp. 4.1–4.14). AGARD CP-295, Neuilly-sur-Seine.

Daly, P. W., Saunders, M. A., Russell, C. T., Rijnbeek, R. P., Sckopke, N., & Russell, C. T. (1984). The distribution of reconnection geometry in flux transfer events using energetic ion, plasma and magnetic data. *Journal of Geophysical Research*, *89*, 3843–3854. https://doi.org/10.1029/JA089iA06p03843

Daly, P. W., Williams, D. J., Russell, C. T., & Keppler, E. (1981). Particle signature of magnetic flux transfer events at the magnetopause. *Journal of Geophysical Research*, *86*, 1628–1632. https://doi.org/10.1029/JA086iA03p01628

Dungey, J. W. (1961). Interplanetary magnetic field and the auroral zones. *Physical Review Letters*, *6*, 47–48. https://doi.org/10.1103/PhysRevLett.6.47

Dunlop, M. W., Zhang, Q.-H., Bogdanova, Y. V., Lockwood, M., Pu, Z., Hasegawa, H., … Liu, Z.-X. (2011). Extended magnetic reconnection across the dayside magnetopause. *Physical Review Letters*, *107*, 25004. https://doi.org/10.1103/PhysRevLett.107.025004

Dunlop, M. W., Zhang, Q. H., Bogdanova, Y. V., Trattner, K. J., Pu, Z., Hasegawa, H., … Carr, C. (2011). Magnetopause reconnection across wide local time. *Annales Geophysicae*, *29*, 1683–1697. https://doi.org/10.5194/angeo-29-1683-2011

Eastwood, J. P., Phan, T. D., Cassak, P. A., Gershman, D. J., Haggerty, C., Malakit, K., … Wang, S. (2016). Ion-scale secondary flux ropes generated by magnetopause reconnection as resolved by MMS. *Geophysical Research Letters*, *43*, 4716–4724. https://doi.org/10.1002/2016GL068747

Eastwood, J. P., Phan, T. D., Fear, R. C., Sibeck, D. G., Angelopoulos, V., Øieroset, M., & Shay, M. A. (2012). Survival of flux transfer event (FTE) flux ropes far along the tail magnetopause. *Journal of Geophysical Research*, *117*, A08222. https://doi.org/10.1029/2012JA017722

Elphic, R. C., Lockwood, M., Cowley, S. W. H., & Sandholt, P. E. (1990). Flux transfer events at the magnetopause and in the ionosphere. *Geophysical Research Letters*, *17*, 2241–2244. https://doi.org/10.1029/GL017i012p02241

Farrugia, C. J., Chen, L. J., Torbert, R. B., Southwood, D. J., Cowley, S. W. H., Vrublevskis, A., … Smith, C. W. (2011). "Crater" flux transfer events: Highroad to the X line? *Journal of Geophysical Research*, *116*, A02204. https://doi.org/10.1029/2010JA015495

Farrugia, C. J., Lavraud, B., Torbert, R. B., Argall, M., Kacem, I., Yu, W., … Strangeway, R. J. (2016). Magnetospheric Multiscale Mission observations and non force free modeling of a flux transfer event immersed in a super-Alfvénic flow. *Geophysical Research Letters*, *43*, 6070–6077. https://doi.org/10.1002/2016GL068758

Farrugia, C. J., Rijnbeek, R. P., Saunders, M. A., Southwood, D. J., Rodgers, D. J., Smith, M. F., … Woolliscroft, L. J. C. (1988). A multi-instrument study of flux transfer event structure. *Journal of Geophysical Research*, *93*, 14,465–14,477. https://doi.org/10.1029/JA093iA12p14465

Fear, R. C., & Milan, S. E. (2012). The IMF dependence of the local time of transpolar arcs: Implications for formation mechanism. *Journal of Geophysical Research*, *117*, A03213. https://doi.org/10.1029/2011JA017209

Fear, R. C., Milan, S. E., Fazakerley, A. N., Fornaçon, K.-H., Carr, C. M., & Dandouras, I. (2009). Simultaneous observations of flux transfer events by THEMIS, Cluster, Double Star, and SuperDARN: Acceleration of FTEs. *Journal of Geophysical Research*, *114*, A10213. https://doi.org/10.1029/2009JA014310

Fear, R. C., Milan, S. E., Fazakerley, A. N., Lucek, E. A., Cowley, S. W. H., & Dandouras, I. (2008). The azimuthal extent of three flux transfer events. *Annales Geophysicae*, *26*, 2353–2369. https://doi.org/10.5194/angeo-26-2353-2008

Fear, R. C., Milan, S. E., Fazakerley, A. N., Owen, C. J., Asikainen, T., Taylor, M. G. G. T., … Daly, P. W. (2007). Motion of flux transfer events: A test of the Cooling model. *Annales Geophysicae*, *25*, 1669–1690. https://doi.org/10.5194/angeo-25-1669-2007

Fear, R. C., Milan, S. E., Lucek, E. A., Cowley, S. W. H., & Fazakerley, A. N. (2010). Mixed azimuthal scales of flux transfer events. In H. Laakso, M. Taylor, & C. P. Escoubet (Eds.), *The Cluster Active Archive — Studying the Earth's space plasma environment, Astrophysics and Space Science Proceedings* (pp. 389–398). Dordrecht, Netherlands: Springer. https://doi.org/10.1007/978-90-481-3499-1_27

Fear, R. C., Milan, S. E., & Oksavik, K. (2012). Determining the axial direction of high-shear flux transfer events: Implications for models of FTE structure. *Journal of Geophysical Research*, *117*, A09220. https://doi.org/10.1029/2012JA017831

Fear, R. C., Palmroth, M., & Milan, S. E. (2012). Seasonal and clock angle control of the location of flux transfer event signatures at the magnetopause. *Journal of Geophysical Research*, *117*, A04202. https://doi.org/10.1029/2011JA017235

Gloag, J. M., Lucek, E. A., Alconcel, L.-N., Balogh, A., Brown, P., Carr, C. M., … Soucek, J. (2010). FGM data products in the CAA. In H. Laakso, M. Taylor, & P. Escoubet (Eds.), *The Cluster Active Archive — Studying the Earth's space plasma environment, Astrophysics and Space Science Proceedings* (pp. 109–128). Dordrecht, Netherlands: Springer. https://doi.org/10.1007/978-90-481-3499-1_7

Greenwald, R. A., Baker, K. B., Dudeney, J. R., Pinnock, M., Jones, T. B., Thomas, E. C., … Yamagishi, H. (1995). DARN/SuperDARN: A global view of high-latitude convection. *Space Science Reviews*, *71*, 761–796. https://doi.org/10.1007/BF00751350

Haerendel, G., Paschmann, G., Sckopke, N., Rosenbauer, H., & Hedgecock, P. C. (1978). The frontside boundary layer of the magnetosphere and the problem of reconnection. *Journal of Geophysical Research*, *83*, 3195–3216. https://doi.org/10.1029/JA083iA07p03195

Harvey, C. C. (1998). Spatial gradients and the volumetric tensor. In G. Paschmann, & P. W. Daly (Eds.), *Analysis methods for multi-spacecraft data* (pp. 307–348). Bern: ISSI.

Hasegawa, H., Kitamura, N., Saito, Y., Nagai, T., Shinohara, I., Yokota, S., … Hesse, M. (2016). Decay of mesoscale flux transfer events during quasi-continuous spatially extended reconnection at the magnetopause. *Geophysical Research Letters*, *43*, 4755–4762. https://doi.org/10.1002/2016GL069225

Hasegawa, H., Sonnerup, B. U. Ö., Owen, C. J., Klecker, B., Paschmann, G., Balogh, A., & Rème, H. (2006). The structure of flux transfer events recovered from Cluster data. *Annales Geophysicae*, *24*, 603–618. https://doi.org/10.5194/angeo-24-603-2006

Hasegawa, H., Wang, J., Dunlop, M. W., Pu, Z. Y., Zhang, Q.-H., Lavraud, B., … Bogdanova, Y. V. (2010). Evidence for a flux transfer event generated by multiple X-line reconnection at the magnetopause. *Geophysical Research Letters*, *37*, L16101. https://doi.org/10.1029/2010GL044219

Huang, C.-S., DeJong, A. D., & Cai, X. (2009). Magnetic flux in the magnetotail and polar cap during sawteeth, isolated substorms, and steady magnetospheric convection events. *Journal of Geophysical Research*, *114*, A07202. https://doi.org/10.1029/2009JA014232

Hwang, K.-J., Sibeck, D. G., Giles, B. L., Pollock, C. J., Gershman, D., Avanov, L., … Burch, J. L. (2016). The substructure of a flux transfer event observed by the MMS spacecraft. *Geophysical Research Letters*, *43*, 9434–9443. https://doi.org/10.1002/2016GL070934

Imber, S. M., Slavin, J. A., Boardsen, S. A., Anderson, B. J., Korth, H., McNutt, R. L., & Solomon, S. C. (2014). MESSENGER observations of large dayside flux transfer events: Do they drive Mercury's substorm cycle?. *Journal of Geophysical Research: Space Physics*, *119*, 5613–5623. https://doi.org/10.1002/2014JA019884

King, J. H., & Papitashvili, N. E. (2005). Solar wind spatial scales in and comparisons of hourly Wind and ACE plasma and magnetic field data. *Journal of Geophysical Research*, *110*, A02104. https://doi.org/10.1029/2004JA010649

Kivelson, M. G., & Khurana, K. K. (1995). Models of flux ropes embedded in a Harris neutral sheet: Force-free solutions in low and high beta plasmas. *Journal of Geophysical Research*, *100*, 23,637–23,645. https://doi.org/10.1029/95JA01548

Korotova, G. I., Sibeck, D. G., & Rosenberg, T. (2008). Seasonal dependence of Interball flux transfer events. *Geophysical Research Letters*, *35*, L05106. https://doi.org/10.1029/2008GL033254

Lee, L. C., & Fu, Z. F. (1985). A theory of magnetic flux transfer at the Earth's magnetopause. *Geophysical Research Letters*, *12*, 105–108. https://doi.org/10.1029/GL012i002p00105

Lockwood, M., Cowley, S. W. H., Sandholt, P. E., & Lepping, R. P. (1990). The ionospheric signatures of flux transfer events and solar wind dynamic pressure changes. *Journal of Geophysical Research*, *95*, 17,113–17,135. https://doi.org/10.1029/JA095iA10p17113

Lockwood, M., Cowley, S. W. H., Smith, M. F., Rijnbeek, R. P., & Elphic, R. C. (1995). The contribution of flux transfer events to convection. *Geophysical Research Letters*, *22*, 1185–1188. https://doi.org/10.1029/95GL01008

Lockwood, M., & Hapgood, M. A. (1998). On the cause of a magnetospheric flux transfer event. *Journal of Geophysical Research*, *103*, 26,453–26,478. https://doi.org/10.1029/98JA02244

Lockwood, M., & Wild, M. N. (1993). On the quasi-periodic nature of magnetopause flux transfer events. *Journal of Geophysical Research*, *98*, 5935–5940. https://doi.org/10.1029/92JA02375

Marchaudon, A., Cerisier, J.-C., Bosqued, J.-M., Dunlop, M. W., Wild, J. A., Décréau, P. M. E., … Laakso, H. (2004). Transient plasma injections in the dayside magnetosphere: One-to-one correlated observations by Cluster and SuperDARN. *Annales Geophysicae*, *22*, 141–158. https://doi.org/10.5194/angeo-22-141-2004

Marchaudon, A., Cerisier, J. C., Greenwald, R. A., & Sofko, G. J. (2004). Electrodynamics of a flux transfer event: Experimental test of the Southwood model. *Geophysical Research Letters*, *31*, L09809. https://doi.org/10.1029/2004GL019922

Marchaudon, A., Owen, C. J., Bosqued, J.-M., Fear, R. C., Fazakerley, A. N., Dunlop, M. W., … Rème, H. (2005). Simultaneous Double Star and Cluster FTEs observations on the dawnside flank of the magnetosphere. *Annales Geophysicae*, *23*, 2877–2887. https://doi.org/10.5194/angeo-23-2877-2005

McComas, D. J., Bame, S. J., Barker, P., Feldman, W. C., Phillips, J. L., Riley, P., & Griffee, J. W. (1998). Solar Wind Electron Proton Alpha Monitor (SWEPAM) for the Advanced Composition Explorer. *Space Science Reviews*, *86*, 563–612. https://doi.org/10.1023/A:1005040232597

McWilliams, K. A., Yeoman, T. K., & Provan, G. (2000). A statistical survey of dayside pulsed ionospheric flows as seen by the CUTLASS Finland HF radar. *Annales Geophysicae*, *18*, 445–453. https://doi.org/10.1007/s005850050902

McWilliams, K. A., Yeoman, T. K., Sibeck, D. G., Milan, S. E., Sofko, G. J., Nagai, T., … Rich, F. J. (2004). Simultaneous observations of magnetopause flux transfer events and of their associated signatures at ionospheric altitudes. *Annales Geophysicae*, *22*, 2181–2199. https://doi.org/10.5194/angeo-22-2181-2004

Milan, S. E., Lester, M., Cowley, S. W. H., Moen, J., Sandholt, P. E., & Owen, C. J. (1999). Meridian-scanning photometer, coherent HF radar, and magnetometer observations of the cusp: A case study. *Annales Geophysicae*, *17*, 159–172. https://doi.org/10.1007/s00585-999-0159-5

Milan, S. E., Imber, S. M., Carter, J. A., Walach, M.-T., & Hubert, B. (2016). What controls the local time extent of flux transfer events. *Journal of Geophysical Research: Space Physics*, *121*, 1391–1401. https://doi.org/10.1002/2015JA022012

Milan, S. E., Lester, M., Cowley, S. W. H., & Brittnacher, M. (2000). Convection and auroral response to a southward turning of the IMF: Polar UVI, CUTLASS, and IMAGE signatures of transient magnetic flux transfer at the magnetopause. *Journal of Geophysical Research*, *105*, 15,741–15,755. https://doi.org/10.1029/2000JA900022

Milan, S. E., Lester, M., Greenwald, R. A., & Sofko, G. (1999). The ionospheric signature of transient dayside reconnection and the associated pulsed convection return flow. *Annales Geophysicae*, *17*, 1166–1171. https://doi.org/10.1007/s00585-999-1166-2

Milan, S. E., Provan, G., & Hubert, B. (2007). Magnetic flux transport in the Dungey cycle: A survey of dayside and nightside reconnection rates. *Journal of Geophysical Research*, *112*, A01209. https://doi.org/10.1029/2006JA011642

Milan, S. E., Yeoman, T. K., Lester, M., Thomas, E. C., & Jones, T. B. (1997). Initial backscatter occurrence statistics from the CUTLASS HF radars. *Annales Geophysicae*, *15*, 703–718. https://doi.org/10.1007/s005850050486

Moen, J., Sandholt, P. E., Lockwood, M., Denig, W. F., Løvhaug, U. P., Lybekk, B., … Friis-Christensen, E. (1995). Events of enhanced convection and related dayside auroral activity. *Journal of Geophysical Research*, *100*, 23,917–23,934. https://doi.org/10.1029/95JA02585

Neudegg, D. A., Cowley, S. W. H., McWilliams, K. A., Lester, M., Yeoman, T. K., Sigwarth, J., … Georgescu, E. (2001). The UV aurora and ionospheric flows during flux transfer events. *Annales Geophysicae*, *19*, 179–188. https://doi.org/10.5194/angeo-19-179-2001

Neudegg, D. A., Cowley, S. W. H., Milan, S. E., Yeoman, T., Lester, M., Provan, G., … Georgescu, E. (2000). A survey of magnetopause FTEs and associated flow bursts in the polar ionosphere. *Annales Geophysicae*, *18*, 416–435. https://doi.org/10.1007/s00585-000-0416-0

Newell, P. T., & Sibeck, D. G. (1993). Upper limits on the contribution of flux transfer events to ionospheric convection. *Geophysical Research Letters*, *20*, 2829–2832. https://doi.org/10.1029/93GL02843

Øieroset, M., Phan, T. D., Eastwood, J. P., Fujimoto, M., Daughton, W., Shay, M. A., … Glassmeier, K.-H. (2011). Direct evidence for a three-dimensional magnetic flux rope flanked by two active magnetic reconnection X lines at Earth's magnetopause. *Physical Review Letters*, *107*(165007). https://doi.org/10.1103/PhysRevLett.107.165007

Oksavik, K., Moen, J., Carlson, H. C., Greenwald, R. A., Milan, S. E., Lester, M., … Barnes, R. J. (2005). Multi-instrument mapping of the small-scale flow dynamics related to a cusp auroral transient. *Annales Geophysicae*, *23*, 2657–2670. https://doi.org/10.5194/angeo-23-2657-2005

Owen, C. J., Marchaudon, A., Dunlop, M. W., Fazakerley, A. N., Bosqued, J.-M., Dewhurst, J. P., … Rème, H. (2008). Cluster observations of crater flux transfer events at the dayside high-latitude magnetopause. *Journal of Geophysical Research*, *113*, A07S04. https://doi.org/10.1029/2007JA012701

Paschmann, G., Haerendel, G., Papamastorakis, I., Sckopke, N., Bame, S. J., Gosling, J. T., & Russell, C. T. (1982). Plasma and magnetic field characteristics of magnetic flux transfer events. *Journal of Geophysical Research*, *87*, 2159–2168. https://doi.org/10.1029/JA087iA04p02159

Paschmann, G., Sonnerup, B. U. Ö., Papamastorakis, I., Sckopke, N., Haerendel, G., Bame, S. J., … Elphic, R. C. (1979). Plasma acceleration at the Earth's magnetopause: Evidence for reconnection. *Nature*, *282*, 243–246. https://doi.org/10.1038/282243a0

Phan, T. D., Kistler, L. M., Klecker, B., Haerendel, G., Paschmann, G., Sonnerup, B. U. Ö., … Rème, H. (2000). Extended magnetic reconnection at the Earth's magnetopause from detection of bi-directional jets. *Nature*, *404*, 848–850. https://doi.org/10.1038/35009050

Pinnock, M., Rodger, A. S., Dudeney, J. R., Baker, K. B., Newell, P. T., Greenwald, R. A., & Greenspan, M. E. (1993). Observations of an enhanced convection channel in the cusp ionosphere. *Journal of Geophysical Research*, *98*, 3767–3776. https://doi.org/10.1029/92JA01382

Pinnock, M., Rodger, A. S., Dudeney, J. R., Rich, F., & Baker, K. B. (1995). High spatial and temporal resolution observations of the ionospheric cusp. *Annales Geophysicae*, *13*, 919–925. https://doi.org/10.1007/s00585-995-0919-9

Provan, G., & Yeoman, T. K. (1999). Statistical observations of the MLT, latitude and size of pulsed ionospheric flows with the CUTLASS Finland radar. *Annales Geophysicae*, *17*, 855–867. https://doi.org/10.1007/s00585-999-0855-1

Provan, G., Yeoman, T. K., & Cowley, S. W. H. (1999). The influence of the IMF By component on the location of pulsed flows in the dayside ionosphere observed by an HF radar. *Geophysical Research Letters*, *26*, 521–524. https://doi.org/10.1029/1999GL900009

Provan, G., Yeoman, T. K., & Milan, S. E. (1998). CUTLASS Finland radar observations of the ionospheric signatures of flux transfer events and the resulting plasma flows. *Annales Geophysicae*, *16*, 1411–1422. https://doi.org/10.1007/s00585-998-1411-0

Rae, I. J., Fenrich, F. R., Lester, M., McWilliams, K. A., & Scudder, J. D. (2004). Solar wind modulation of cusp particle signatures and their associated ionospheric flows. *Journal of Geophysical Research*, *109*, A03223. https://doi.org/10.1029/2003JA010188

Raeder, J. (2006). Flux transfer events: 1. Generation mechanism for strong southward IMF. *Annales Geophysicae*, *24*, 381–392.

Rijnbeek, R. P., & Cowley, S. W. H. (1984). Magnetospheric flux erosion events are flux transfer events. *Nature*, *309*, 135–138. https://doi.org/10.1038/309135a0

Rijnbeek, R. P., Cowley, S. W. H., Southwood, D. J., & Russell, C. T. (1982). Observations of reverse polarity flux transfer events at the Earth's dayside magnetopause. *Nature*, *300*, 23–26. https://doi.org/10.1038/300023a0

Rijnbeek, R. P., Cowley, S. W. H., Southwood, D. J., & Russell, C. T. (1984). A survey of dayside transfer events observed by ISEE 1 and 2 magnetometers. *Journal of Geophysical Research*, *89*, 786–800. https://doi.org/10.1029/JA089iA02p00786

Rong, Z. J., Lui, A. T. Y., Wan, W. X., Yang, Y. Y., Shen, C., Petrukovich, A. A., … Wei, Y. (2015). Time delay of interplanetary magnetic field penetration into Earth's magnetotail. *Journal of Geophysical Research: Space Physics*, *120*, 3406–3414. https://doi.org/10.1002/2014JA020452

Ruohoniemi, J. M., & Baker, K. B. (1998). Large-scale imaging of high-latitude convection with Super Dual Auroral Radar Network HF radar observations. *Journal of Geophysical Research*, *103*, 20,797–20,811. https://doi.org/10.1029/98JA01288

Russell, C. T., & Elphic, R. C. (1978). Initial ISEE magnetometer results: Magnetopause observations. *Space Science Reviews*, *22*, 681–715. https://doi.org/10.1007/BF00212619

Russell, C. T., & Elphic, R. C. (1979). ISEE observations of flux transfer events at the dayside magnetopause. *Geophysical Research Letters*, *6*, 33–36. https://doi.org/10.1029/GL006i001p00033

Russell, C. T., & Walker, R. J. (1985). Flux transfer events at Mercury. *Journal of Geophysical Research*, *90*, 11,067–11,074. https://doi.org/10.1029/JA090iA11p11067

Sandholt, P. E., Deehr, C. S., Egeland, A., Lybekk, B., Viereck, R., & Romick, G. J. (1986). Signatures in the dayside aurora of plasma transfer from the magnetosheath. *Journal of Geophysical Research*, *91*, 10,063–10,079. https://doi.org/10.1029/JA091iA09p10063

Sandholt, P. E., Lockwood, M., Denig, W. F., Elphic, R. C., & Leontjev, S. (1992). Dynamical auroral structure in the vicinity of the polar cusp: Multipoint observations during southward and northward IMF. *Annales Geophysicae*, *10*, 483–497.

Saunders, M. A., Russell, C. T., & Sckopke, N. (1984). Flux transfer events: Scale size and interior structure. *Geophysical Research Letters*, *11*, 131–134. https://doi.org/10.1029/GL011i002p00131

Scholer, M. (1988). Magnetic flux transfer at the magnetopause based on single X line bursty reconnection. *Geophysical Research Letters*, *15*, 291–294. https://doi.org/10.1029/GL015i004p00291

Shue, J.-H., Song, P., Russell, C. T., Steinberg, J. T., Chao, J. K., Zastenker, G., … Kawano, H. (1998). Magnetopause location under extreme solar wind conditions. *Journal of Geophysical Research*, *103*, 17,691–17,700. https://doi.org/10.1029/98JA01103

Slavin, J. A., Imber, S. M., Boardsen, S. A., DiBraccio, G. A., Sundberg, T., Sarantos, M., … Solomon, S. C. (2012). MESSENGER observations of a flux-transfer-event shower at Mercury. *Journal of Geophysical Research*, *117*, A00M06. https://doi.org/10.1029/2012JA017926

Slavin, J. A., Lepping, R. P., Gjerloev, J., Fairfield, D. H., Hesse, M., Owen, C. J., … Mukai, T. (2003). Geotail observations of magnetic flux ropes in the plasma sheet. *Journal of Geophysical Research*, *108*, 1015. https://doi.org/10.1029/2002JA009557

Slavin, J. A., Lepping, R. P., Wu, C.-C., Anderson, B. J., Baker, D. N., Benna, M., … Zurbuchen, T. H. (2010). MESSENGER observations of large flux transfer events at Mercury. *Geophysical Research Letters*, *37*, L02105. https://doi.org/10.1029/2009GL041485

Smith, C. W., L'Heureux, J., Ness, N. F., Acuña, M. H., Burlaga, L. F., & Scheifele, J. (1998). The ACE magnetic fields experiment. *Space Science Reviews*, *86*, 613–632. https://doi.org/10.1023/A:1005092216668

Sonnerup, B. U. Ö., Hasegawa, H., & Paschmann, G. (2004). Anatomy of a flux transfer event seen by Cluster. *Geophysical Research Letters*, *31*, L11803. https://doi.org/10.1029/2004GL020134

Southwood, D. J., Farrugia, C. J., & Saunders, M. A. (1988). What are flux transfer events?. *Planetary and Space Science*, *36*, 503–508. https://doi.org/10.1016/0032-0633(88)90109-2

Thomsen, M. F., Stansberry, J. A., Bame, S. J., Fuselier, S. A., & Gosling, J. T. (1987). Ion and electron velocity distributions within flux transfer events. *Journal of Geophysical Research*, *92*, 12,127–12,136. https://doi.org/10.1029/JA092iA11p12127

Trattner, K. J., Thresher, S., Trenchi, L., Fuselier, S. A., Petrinec, S. M., Peterson, W. K., & Marcucci, M. F. (2017). On the occurrence of magnetic reconnection equatorward of the cusps at the Earth's magnetopause during northward IMF conditions. *Journal of Geophysical Research: Space Physics*, *122*, 605–617. https://doi.org/10.1002/2016JA023398

Trenchi, L., Fear, R. C., Trattner, K. J., Mihaljcic, B., & Fazakerley, A. N. (2016). A sequence of flux transfer events potentially generated by different generation mechanisms. *Journal of Geophysical Research: Space Physics*, *121*, 8624–8639. https://doi.org/10.1002/2016JA022847

Trenchi, L., Marcucci, M. F., Rème, H., Carr, C. M., & Cao, J. B. (2011). TC-1 observations of a flux rope: Generation by multiple X line reconnection. *Journal of Geophysical Research*, *116*, A05202. https://doi.org/10.1029/2010JA015986

Tsyganenko, N. A. (1996). Effects of the solar wind conditions on the global magnetospheric configuration as deduced from data-based field models. In *Proc. Third International Conference on Substorms (ICS-3)* (pp. 181–185). ESA SP-389, Paris.

Varsani, A., Owen, C. J., Fazakerley, A. N., Forsyth, C., Walsh, A. P., André, M., … Carr, C. M. (2014). Cluster observations of the substructure of a flux transfer event: Analysis of high-time-resolution particle data. *Annales Geophysicae*, *32*, 1093–1117. https://doi.org/10.5194/angeo-32-1093-2014

Wild, J. A., Cowley, S. W. H., Davies, J. A., Khan, H., Lester, M., Milan, S. E., … Georgescu, E. (2001). First simultaneous observations of flux transfer events at the high-latitude magnetopause by the Cluster spacecraft and pulsed radar signatures in the conjugate ionosphere by the CUTLASS and EISCAT radars. *Annales Geophysicae*, *19*, 1491–1508. https://doi.org/10.5194/angeo-19-1491-2001

Wild, J. A., Milan, S. E., Davies, J. A., Dunlop, M. W., Wright, D. M., Carr, C. M., … Marchaudon, A. (2007). On the location of dayside magnetic reconnection during an interval of duskward oriented IMF. *Annales Geophysicae*, *25*, 219–238. https://doi.org/10.5194/angeo-25-219-2007

Wild, J. A., Milan, S. E., Cowley, S. W. H., Dunlop, M. W., Owen, C. J., Bosqued, J. M., … Rème, H. (2003). Coordinated interhemispheric SuperDARN radar observations of the ionospheric response to flux transfer events observed by the Cluster spacecraft at the high-latitude magnetopause. *Annales Geophysicae*, *21*, 1807–1826. https://doi.org/10.5194/angeo-21-1807-2003

Wild, J. A., Milan, S. E., Davies, J. A., Cowley, S. W. H., Carr, C. M., & Balogh, A. (2005). Double Star, Cluster, and ground-based observations of magnetic reconnection during an interval of duskward oriented IMF: Preliminary results. *Annales Geophysicae*, *23*, 2903–2907. https://doi.org/10.5194/angeo-23-2903-2005

Zhang, H., Khurana, K. K., Kivelson, M. G., Angelopoulos, V., Pu, Z. Y., Zong, Q.-G., … Zhou, X.-Z. (2008). Modeling a force-free flux transfer event probed by multiple Time History of Events and Macroscale Interactions during Substorms (THEMIS) spacecraft. *Journal of Geophysical Research*, *113*, A00C05. https://doi.org/10.1029/2008JA013451

Zhang, Q.-H., Lockwood, M., Foster, J. C., Zhang, S.-R., Zhang, B.-C., McCrea, I. W., … Ruohoniemi, J. M. (2015). Direct observations of the full Dungey convection cycle in the polar ionosphere for southward interplanetary magnetic field conditions. *Journal of Geophysical Research: Space Physics*, *120*, 4519–4530. https://doi.org/10.1002/2015JA021172

Zhao, C., Russell, C. T., Strangeway, R. J., Petrinec, S. M., Paterson, W. R., Zhou, M., … Wei, H. Y. (2016). Force balance at the magnetopause determined with MMS: Application to flux transfer events. *Geophysical Research Letters*, *43*, 11,941–11,947. https://doi.org/10.1002/2016GL071568